Impaired Urea Accumulation in the Inner Medulla of Mice Lacking the Urea Transporter UT-A2

Shinichi Uchida,[1]* Eisei Sohara,[1] Tatemitsu Rai,[1] Masahito Ikawa,[2] Masaru Okabe,[2] and Sei Sasaki[1]

Department of Nephrology, Graduate School of Medicine, Tokyo Medical and Dental University, Tokyo,[1] and Genome Information Research Center, Osaka University, Osaka,[2] Japan

Urea transporter UT-A2, the major urea transporter of the thin descending limb of the loop of Henle in short loop nephrons, has been implicated in urea recycling in the medulla, thereby producing concentrated urine. To investigate the physiological role of UT-A2 in vivo, we generated UT-A2-selective knockout mice by deleting the UT-A2 promoter. Western analysis, immunohistochemistry, and quantitative reverse transcription-PCR were used to confirm the specific deletion of UT-A2 with preservation of other UT-A transporters. Compared to wild-type mice, differences in the urine outputs of UT-A2$^{-/-}$ mice consuming a normal protein diet (20% protein) were not observed under normal conditions or with dehydration. Likewise, impairment of urea accumulation in the inner medulla of UT-A2$^{-/-}$ mice was not observed. On a low-protein diet (4% protein), however, significantly reduced maximal urine osmolality was observed in dehydrated UT-A2$^{-/-}$ mice compared to wild-type littermates (2,500 mosmol versus 3,450 mosmol, respectively). A significant reduction in urea accumulation in the inner medulla was also observed in UT-A2$^{-/-}$ mice; however, differences in Na$^+$ and Cl$^-$ accumulation were not observed. Thus, UT-A2 is important for maintaining a high concentration of urea in the inner medulla when urea supply to the kidney is limited.

Urea transport in the renal medullary epithelium may generate a high urea concentration in the inner medulla, thereby contributing to a urine concentration mechanism (11). Molecular cloning technology has identified a number of genes encoding transepithelial urea transport proteins (3, 7–9, 16–18, 26). In mammals, two distinct urea transporter genes have been identified (16, 26). One is UT-B, which encodes a urea transporter expressed by erythrocytes and endothelial cells (16). Within the kidney, UT-B is expressed by endothelial cells of the descending vasa recta of the medulla, and it is thought to be important in the recycling of urea between the descending and ascending vasa recta (23). This countercurrent exchange of urea is thought to maintain a high concentration of urea in the inner medulla. Recently, UT-B knockout mice have been shown to have a reduced ability to concentrate urine, which supports the role of countercurrent exchange of urea in producing concentrated urine (5, 25). The second mammalian urea transporter gene is UT-A. Five UT-A isoforms have been identified (UT-A1 to UT-A5), all of which are produced by alternate splicing of a single gene (2–4). One of these isoforms, UT-A1 (originally named UT1), is expressed by terminal inner medullary collecting ducts and is thought to mediate vasopressin-induced increases in urea permeability (15). UT-A3 is also present in terminal collecting ducts (9, 21, 22), and UT-A1 and UT-A3 are thought to share a common promoter (2). Recently, UT-A1/A3 knockout mice have been produced by deleting exons common to UT-A1 and UT-A3 (6). These knockout mice are unable to accumulate urea in the inner medulla and have a reduced ability to concentrate urine.

Although UT-A2 shares several exons with UT-A1, transcription of UT-A2 is governed by a different promoter than UT-A1, UT-A3, or UT-A4 (2, 14). Its intrarenal localization also differs from that of UT-A1, UT-A3, or UT-A4. Under normal conditions of hydration, UT-A2 is found in the lower portion of the thin descending limb of short-looped nephrons (8, 24). A marked increase in UT-A2 expression has been observed in response to dehydration (4, 19, 20) and 1-deamino-8-D-arginine vasopressin (DDAVP) injection (24). This suggests that UT-A2 may also influence the ability to concentrate urine. As well as the "vascular" mechanism of urea recycling mediated by UT-B, countercurrent exchange of urea between the ascending vasa recta and the thin descending loop of Henle (via UT-A2) might function as a "tubular" urea recycling pathway, thereby preventing urea from being washed out from the inner medulla.

To investigate the role of UT-A2 in urea accumulation in the inner medulla and its influence on urine concentration, we deleted ~3 kb of the mouse UT-A2 promoter by gene targeting. Deletion of this segment selectively disrupted expression of UT-A2, while sparing the expression of other kidney UT-A transporters. Surprisingly, in contrast to UT-A1/A3 and UT-B knockout mice, only a mild deficit in urine concentrating ability was observed in UT-A2 knockout mice. This was observed only in the context of limited urea supply to the kidney due to consumption of a low protein diet (4% protein).

MATERIALS AND METHODS

Generation of UT-A2 null mice. Three overlapping lamda clones were isolated from a 129/SVJ mouse genomic DNA library (Stratagene) by plaque hybridization using several exons of the UT-A gene as probes. Long- and short-arm genomic fragments were cut out of the lambda clones and ligated into a pLNTK vector (13). The long- and short-arm fragments contained exons 9 to 12 and intron 13, respectively (see Fig. 1). As a result of homologous recombination, the

* Corresponding author. Mailing address: 1-5-45 Yushima Bunkyo, Tokyo 113-8519, Japan. Phone: 81-3-5803-5214. Fax: 81-3-5803-5215. E-mail: suchida.kid@tmd.ac.jp.
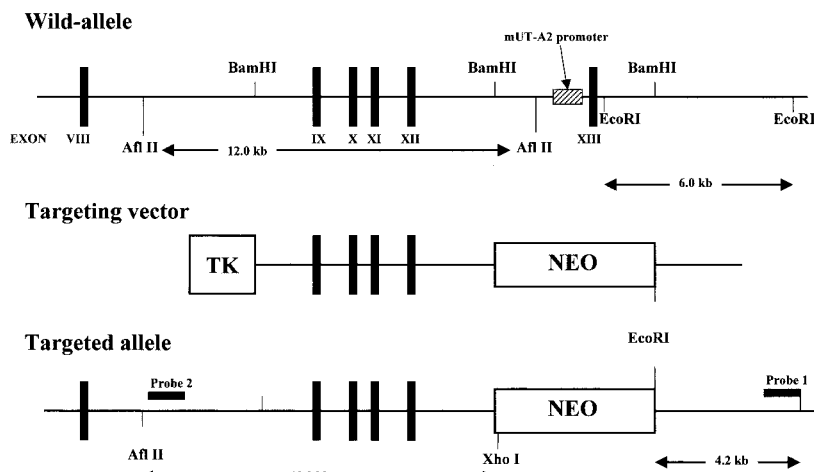
FIG. 1. Gene targeting of mouse UT-A2. Schematic representation of the wild-type UT-A gene, the targeting vector, and the mutant allele after homologous recombination. A 4-kb genomic fragment including the UT-A2 promoter and exon 13 was replaced by a *neo* cassette. There is no XhoI site in the wild-type allele.

UT-A2 promoter and the first noncoding exon of UT-A2, which contained the transcription start site, were presumed deleted. The targeting vector was linearized with SalI and electroporated into D3 embryonic stem cells. Transfected cells were selected by exposure to G418 and ganciclovir for 7 days, after which the isolated colonies were screened by PCR. Homologous recombination was confirmed by Southern hybridization on both long- and short-arm sides, as shown in Fig. 1. Five out of nine clones were chosen after a karyotype test and injected into blastocysts derived from C57BL/6 mice to produce chimeric mice. Chimeric pups were identified by their agouti coat color, after which the chimeric males were bred to C57BL/6J females, and germ line transmission was determined by the coat color of the offspring. Genotyping of the progeny was carried out by Southern blot analysis of tail biopsy genomic DNA. As a result, two independent lines of UT-A2$^{-/-}$ mice were produced exhibiting the phenotypes described below.

Northern blot analysis. Total RNA from mouse whole kidney was isolated using Trizol reagent (Invitrogen), resolved by 1% formaldehyde-agarose gel electrophoresis, and transferred to a nylon membrane (Biodyne B, Pall Corp.). Hybridization was carried out at high stringency with ^{32}P-labeled exons 17 and 19.

Immunohistochemistry and immunoblot analysis. Rabbit antiserum was raised against the 19 carboxy-terminal amino acids (QEKNRRASMITKYQAY DVS) of UT-A1, UT-A2, and UT-A4 (#47), as well as the 14 carboxy-terminal amino acids (TVRRSEEEKSPNGD) of UT-A3 (#57), as previously described (6, 8, 9, 15, 21, 22, 24). Specificities of the affinity-purified antibodies were confirmed by immunoblot and immunohistochemical analysis of wild-type mice, as described in the Results and Discussion section. To prepare cryostat sections, kidneys were perfused and fixed in a PLP solution (6% paraformaldehyde, 25 mM L-lysine monohydrochloride, and 0.1 M sodium periodate in phosphate-buffered saline), after which they were frozen in liquid nitrogen. Immunostaining was performed using anti-UT-A antibodies (1:200 dilution) and Alexa Fluor 546-conjugated anti-rabbit immunoglobulin G antibody. For immunoblot analysis, the outer medulla and papillary region of each mouse kidney were dissected under a microscope and homogenized in phosphate-buffered saline containing 1% Nonidet P-40, 0.5% sodium deoxycholate, 0.1% sodium dodecyl sulfate (SDS), and protease inhibitors (Complete; Roche). The protein samples were resolved by SDS-polyacrylamide gel electrophoresis and transferred to a nitrocellulose membrane (Hibond ECL; Amersham). Signals were detected using anti-UT-A antibodies (1:200 dilution), alkaliphosphatase-conjugated anti-rabbit immunoglobulin G, and Western blue detection reagent (Promega).

Real-time RT-PCR. Primers for real-time reverse transcription (RT) PCR of mouse UT-A1, UT-A2, UT-A3, UT-A4, UT-B, and beta-actin were prepared as previously described (10). Total RNA isolated from whole mouse kidney was reverse transcribed with Omniscript reverse transcriptase (QIAGEN). cDNA was used as a template for real-time PCR. Real-time PCR was carried out in a LightCycler (Roche) using a LightCycler Fast Start DNA Master SYBR Green I kit (Roche).

Metabolic cage studies. Daily urine was collected from mice placed in mouse metabolic cages (Sugiyamagen Iriki). Urine samples were obtained from the mice under basal conditions (unrestricted access to food and water), as well as

after a 36-h deprivation period of food and water. Blood samples were obtained by tail bleeding. Hematocrit, electrolytes, and urea were measured using an i-STAT blood analyzer (i-STAT Corporation). Homogenates of inner medullary tissue were obtained by homogenizing four papillae in 200 μl H$_2$O, after which the supernatant was centrifuged and assayed for urea, sodium, and chloride. Sodium and chloride concentrations were measured using a 9180 Electrolyte Analyzer (AVL Scientific Corporation), and urea concentrations were measured using the urea test (Wako). Osmolality was measured with a One-Ten Osmometer (Fiske). Papillary osmolality, urea, and chloride concentrations were calculated in terms of wet tissue weight.

Statistics. Results obtained from the knockout mice were compared with those of the wild-type littermates using Student's *t* test. A test of multiple comparisons was also performed using one-way analysis of variance. A *P* of <0.05 was considered statistically significant.

RESULTS AND DISCUSSION

Generation of UT-A2-specific knockout mice. UT-A2 knockout mice were generated using the gene-targeting strategy shown in Fig. 1. Based on the previously identified structure of the UT-A gene, we decided to delete the promoter region and first noncoding exon (exon 13) of the UT-A2 gene, since all other UT-A2 exons are also present in UT-A1 (2), but UT-A2 is driven by a different promoter (14). Genomic Southern blot of mouse tail genomic DNA digested with EcoRI (Fig. 2A) produced a 6.0-kb fragment in wild-type mice and a 4.2-kb fragment in UT-A2$^{-/-}$ mice with probe 1 (Fig. 1). Southern blot analysis of genomic DNA cut with AflII and XhoI was also performed with probe 2 (Fig. 1) to confirm UT-A gene structure on the reverse side of the *neo* cassette (Fig. 2B). A 12-kb fragment in wild-type mice and a 10-kb fragment in UT-A2$^{-/-}$ mice were detected. To verify the absence of UT-A2 mRNA in UT-A2$^{-/-}$ mice, Northern blot analysis of total RNA from whole kidney was performed using exons 17 and 19. Although exon 19 is common to UT-A1, UT-A2, and UT-A4 mRNA, only UT-A2 can be detected under these conditions, since the UT-A4 transcript has never been detected by Northern analysis (2, 17), and since the UT-A1 transcript has been detected only when poly(A)$^+$ RNA from whole kidney is used (8). As is clearly shown in Fig. 2C, UT-A2 mRNA was not detected in UT-A2$^{-/-}$ mice. Identical results were obtained using exon 17,
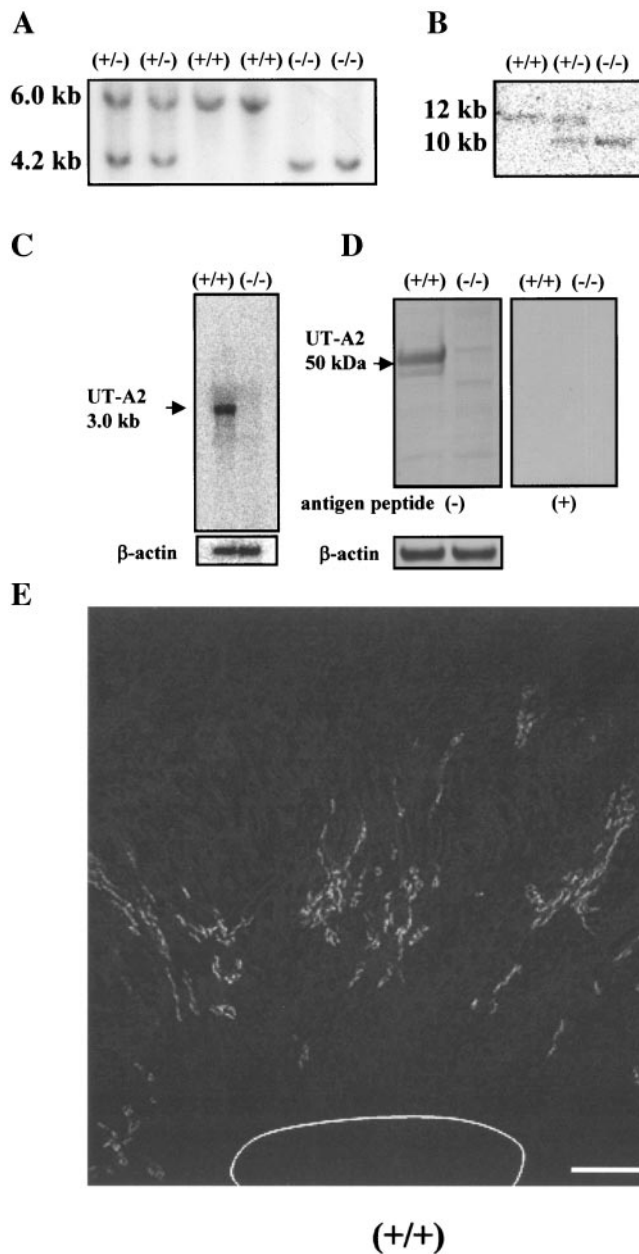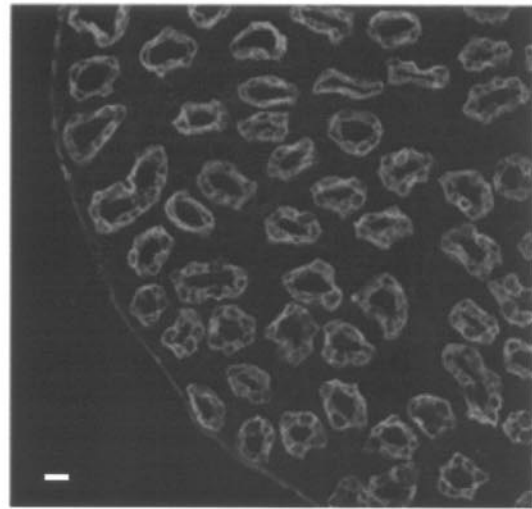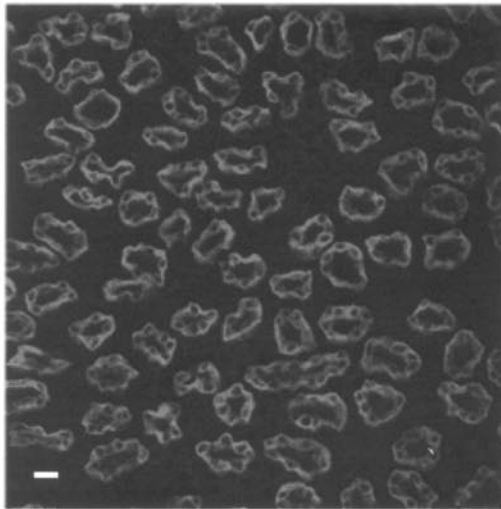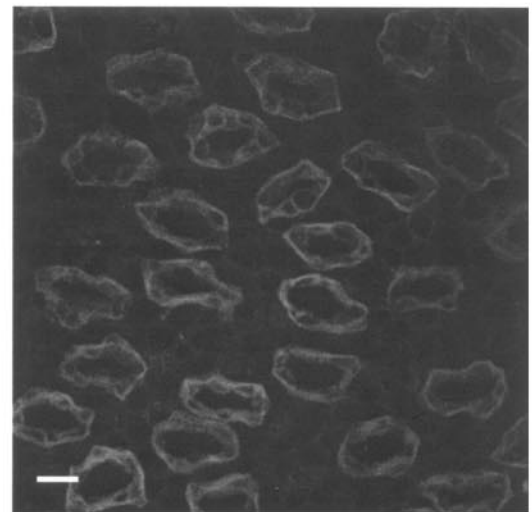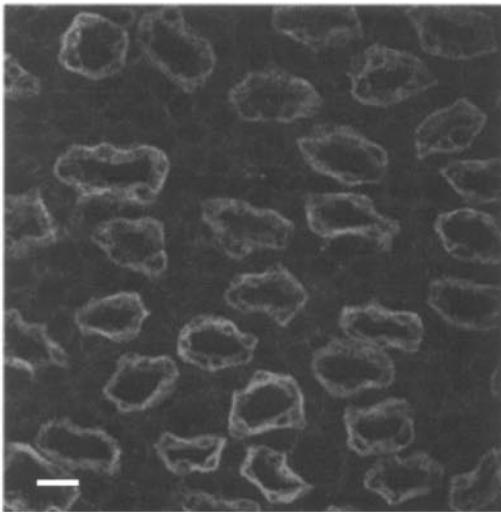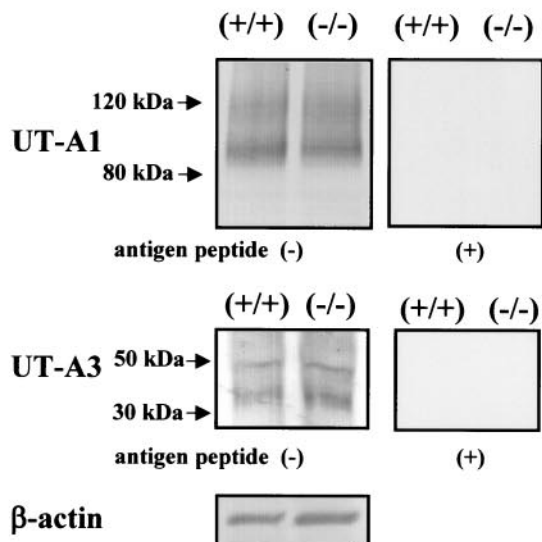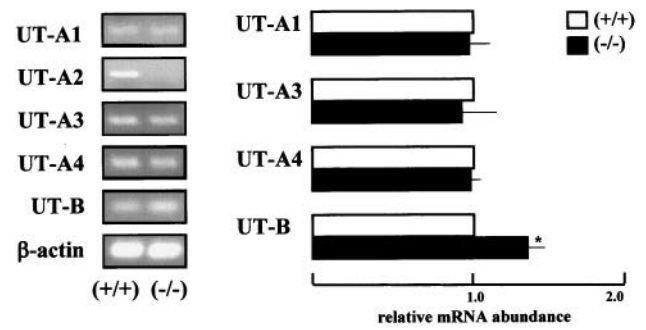
FIG. 2. Generation of UT-A2 null mice. A. Southern blot of mouse tail genomic DNA digested with EcoRI hybridized with probe 1 as indicated in Fig. 1. B. Southern blot of mouse tail genomic DNA double-digested with AflII and XhoI hybridized with probe 2 as indicated in Fig. 1. C. Northern blot of mouse kidney probed with mouse UT-A1 and UT-A2 coding exon 19. The 3-kb UT-A2 signal was absent in UT-A2$^{-/-}$ mice. D. Western blot of mouse outer medulla with affinity-purified anti-UTA1 and UT-A2 antibody (#47). A distinct band of around 50 kDa observed in the outer medulla of wild-type mice was absent in the UT-A2$^{-/-}$ kidney. Preincubation of the antibody with immunizing peptide abolished the 50-kDa band in the wild-type outer medulla. E. Immunofluorescence localization of UT-A2 protein in the outer medulla of wild-type (left) and UT-A2$^{-/-}$ (right) mice. Bar = 200 μm. Intense UT-A2 staining in the outer medulla of wild-type mice was absent in the outer medulla of UT-A2$^{-/-}$ mice. White lines indicate the border between the outer and inner medullas.

which is present in both UT-A1 and UT-A2 mRNA (data not shown). These results confirm that we deleted a region containing a promoter essential for UT-A2 transcription. Figure 2D shows the immunoblot results of outer medullary proteins probed with antibody #47, which recognizes a C-terminal epitope common to UT-A1, UT-A2, and UT-A4. Antibody #47 did react with a 50-kDa outer medullary protein in wild-type mice, previously identified as UT-A2 (8, 24). Specificity of this antibody to UT-A2 was shown by the disappearance of the 50-kDa protein band following preincubation with the immunizing peptide (right panel, Fig. 2D). This 50-kDa protein band was not observed among the outer medullary proteins of UT-A2$^{-/-}$ mice. Immunohistochemistry revealed a complete absence of UT-A2 in UT-A2$^{-/-}$ mice (Fig. 2E). The same anti-

body highlighted the presence UT-A1 in the inner medulla of UT-A2$^{-/-}$ mice (upper panels, Fig. 3A). Similarly, a UT-A3-specific antibody (antibody #57) was used to demonstrate the presence of UT-A3 in the inner medulla of UT-A2$^{-/-}$ mice (lower panels, Fig. 3A). Aberrant staining was not observed using these antibodies in UT-A2$^{-/-}$ mice. The inner medullary protein immunoblot results shown in Fig. 3B confirm that UT-A1 and UT-A3 expression in the inner medulla is not affected by deletion of the UT-A2 promoter of the UT-A gene (left panels) and also confirm the specificities of the antibodies used (right panels).

To enable quantitative measurement of the mRNA levels of various urea transporters among wild-type and UT-A2$^{-/-}$ mice, real-time RT-PCR was performed using whole kidney

A

UT-A1

UT-A3

(+/+)　　　　(-/-)

B

UT-A1

(+/+)　(-/-)　(+/+)　(-/-)

120 kDa →
80 kDa →

antigen peptide (-)　　(+)

UT-A3

(+/+)　(-/-)　(+/+)　(-/-)

50 kDa →
30 kDa →

antigen peptide (-)　　(+)

β-actin

C

UT-A1
UT-A2
UT-A3
UT-A4
UT-B
β-actin

(+/+)　(-/-)

UT-A1
UT-A3
UT-A4
UT-B

□ (+/+)
■ (-/-)
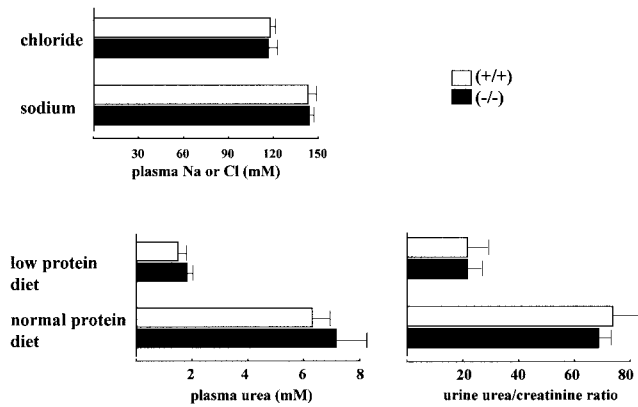
1.0　　　2.0
relative mRNA abundance

FIG. 4. Plasma and urine analysis of UT-A2$^{-/-}$ mice. Plasma sodium and chloride concentrations were measured in mice fed a 20% protein diet under basal conditions (free access to food and water). Plasma and urine urea concentrations were measured in mice fed 20% and 4% protein diets. The data showed no differences between wild-type and UT-A2$^{-/-}$ mice ($n = 5$). Mice were fed a low protein diet for at least 7 days prior to experimentation.

mRNA as the template. As shown in Fig. 3C, UT-A2 mRNA was not detected, thus confirming the results of Northern, immunoblot, and immunohistochemical analyses. Although Klein et al. (10) have reported an inability to detect UT-A4 mRNA using this primer set, we were able to detect UT-A4 mRNA, and no differences in expression were observed among wild-type and UT-A2$^{-/-}$ mice. As the immunoblot and immunohistochemistry results suggest (Fig. 3B), UT-A1 and UT-A3 mRNA levels were not affected by deleting UT-A2 expression. This is reasonable, since these UT-A transporters share a common promoter. Only a slight increase in UT-B mRNA was observed in UT-A2$^{-/-}$ mice. UT-A2 and UT-B are found in close proximity to the ascending vasa recta and in similar locations within nephrons, where they function in urea recycling. Thus, an increase in UT-B mRNA might compensate for a deletion of UT-A2, even though only a slight increase in UT-B mRNA was observed.

Phenotypes of UT-A2$^{-/-}$ mice. UT-A2$^{-/-}$ mice exhibited normal growth and no physiological abnormalities. A normal distribution of genotype ratios was observed among UT-A2$^{-/-}$ mice, suggesting that UT-A2 deletion did not affect development and survival. Crossing of male and female UT-A2$^{-/-}$ mice yielded the same number of offspring as wild-type mice, suggesting no influence of UT-A2 deletion on reproduction.

Since UT-A2 has been implicated in urea recycling (17), and since deletion of UT-B has been shown to result in urea-specific urine concentrating deficits (25), we compared the urine concentrating abilities of wild-type and UT-A2$^{-/-}$ mice. Under basal conditions (free access to food and water), plasma
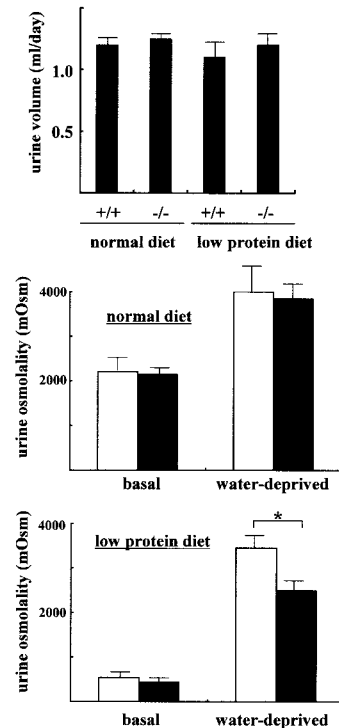

FIG. 5. Urine concentrating ability of UT-A2$^{-/-}$ mice. Upper panel, daily urine output of mice fed normal (20% protein) and low protein (4%) diets under basal conditions (free access to food and water). Middle and lower panels, urine osmolality of mice fed normal (20% protein) and low protein (4%) diets under basal and dehydrated (36-h period of water deprivation) conditions. *, $P < 0.05$; $n = 5$. Filled bars represent $-/-$, and open bars represent $+/+$.

urea, sodium, and chloride concentrations were similar between the two groups (Fig. 4). Significant differences in daily urine output were not observed between the two groups (upper panel, Fig. 5). Even after a 36-h period of water deprivation, differences in urine output and urine osmolality were not observed among wild-type and UT-A2$^{-/-}$ mice (middle panel, Fig. 5). Significantly different data were obtained for UT-B knockout mice. Although UT-B knockout mice exhibited only mild polyuria, they had reduced urea concentrations in their urine and slightly increased plasma levels of urea, as well as significantly decreased urea accumulation in the inner medulla (25). As shown in the lower panels of Fig. 4, plasma urea and urinary excretion of urea were not affected by deletion of UT-A2. The concentrations of urea and chloride within the inner medulla of UT-A2$^{-/-}$ mice (Fig. 6) were also not affected by UT-A2 deletion. This finding was surprising since UT-A2 has been implicated in transporting urea out of the ascending vasa recta, thereby maintaining a high inner medul-

FIG. 3. Expression of other urea transporters. A. Immunofluorescence of UT-A1 and UT-A3 in the inner medulla. Antibodies #47 and #57 recognized UT-A1 and UT-A3, respectively, in the collecting ducts of the inner medulla. Their density and cellular localization did not appear to change in UT-A2 knockout mice. Bar = 20 μm. B. Immunoblots of the inner medulla with antibodies #47 and #57. Antibodies #47 and #57 recognized UT-A1 bands of ~100 and 120 kDa (6), and UT-A3 bands of ~40 and 50 kDa (6), respectively, in inner medulla of wild-type and UT-A2$^{-/-}$ mice. All of these bands were absent following preincubation of the antibodies with the relevant immunizing peptides. C. Real-time RT-PCR analysis of renal urea transporters. Total RNA from whole mouse kidney was used as a starting material. UT-B expression was significantly increased in UT-A2$^{-/-}$ mice. $P < 0.05$, $n = 5$.
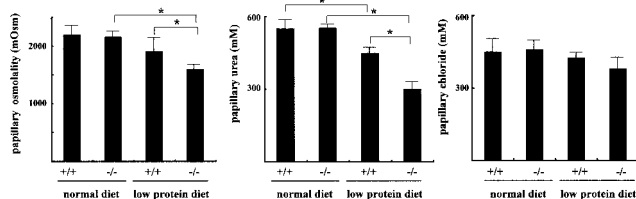
FIG. 6. Papillary tissue osmolality, urea, and chloride concentrations. Papillae were dissected from mice dehydrated for 36 h and homogenized in water. Homogenate concentrations were measured to determine total osmolality, urea, and chloride concentrations within the tissue samples, which were then divided by the wet tissue weight of papillae. Fed a low protein diet, UT-A2$^{-/-}$ mice had reduced papillary osmolality and a reduced medullary urea concentration, compared to wild-type mice. $P < 0.05$, $n = 5$.

lary urea gradient. Up-regulation of UT-A2 mRNA by dehydration (19, 20, 24) and DDAVP (24) infusion, as well as the observed decline in UT-A2 mRNA levels and urine concentration with cyclosporine treatment (12), strongly suggests an important role of UT-A2 in urine concentrating mechanisms. Although a slight increase in UT-B mRNA was observed in UT-A2$^{-/-}$ mice, compensatory increases in UT-A1 and UT-A3 mRNA were not observed. This suggests that the continued ability of UT-A2$^{-/-}$ mice to concentrate urine in the present experiment was not due to a compensatory increase in other urea transporters. Based on these observations, we conclude that UT-A2 makes only a small contribution to urine concentrating mechanisms under normal conditions. Thus, we next tested the ability of UT-A2$^{-/-}$ mice to concentrate urine when the supply of urea to the kidney is limited, for example, in mice fed a low-protein diet (4.0% protein). As shown in Fig. 4, plasma and urine urea concentrations were significantly decreased in both groups of mice fed a low-protein diet. Urine osmolality under basal conditions (free access to food and water) was also decreased in both groups (middle and lower panels, Fig. 5) (538 mosmol in wild-type mice and 438 mosmol in UT-A2$^{-/-}$ mice); however, differences in urine volume and urine osmolality were not observed between wild-type and UT-A2$^{-/-}$ mice (lower panel, Fig. 5). However, after 36 h of dehydration, significantly reduced maximal urine osmolality was observed in UT-A2$^{-/-}$ mice (3,450 ± 180 mosmol versus 2,500 ± 150 mosmol for control versus UT-A2$^{-/-}$ mice, respectively [means ± standard errors, $n = 5$/group]). Significant decreases in total osmolality and urea within the inner medulla were also observed in UT-A2$^{-/-}$ mice (Fig. 6). Although a tendency for decreased average values of sodium and chloride concentrations were also observed, these findings were not statistically significant. This selective reduction in inner medullary urea concentration is consistent with previously reported data involving UT-A1 and UT-A3 (6) and UT-B (25) knockout mice. Previously, we showed that deletion of a chloride channel in the thin ascending limb of the loop of Henle affects both chloride and urea accumulation in the inner medulla (1, 13). A disproportionate reduction in the concentration of urea compared to sodium and chloride concentrations is characteristic of renal urea transporter knockout mice.

This study clearly demonstrates that UT-A2 makes a minimal contribution to urea accumulation in the inner medulla

under basal conditions. Since several lines of evidence suggest a role of UT-A2 in urinary concentrating mechanisms, the results of the present study are surprising. However, this study clearly demonstrates the role of UT-A2 in maintaining a high urea concentration within the inner medulla, thereby producing maximally concentrated urine. This is more likely to occur in wild animals with inadequate daily protein intake than in laboratory animals.

REFERENCES

1. **Akizuki, N., S. Uchida, S. Sasaki, and F. Marumo.** 2001. Impaired solute accumulation in inner medulla of Clcnk1$^{-/-}$ mice kidney. Am. J. Physiol. Renal Physiol. **280:**F79–F87.
2. **Bagnasco, S. M.** 2003. Gene structure of urea transporters. Am. J. Physiol. Renal Physiol. **284:**F3–F10.
3. **Bagnasco, S. M., T. Peng, M. G. Janech, A. Karakashian, and J. M. Sands.** 2001. Cloning and characterization of the human urea transporter UT-A1 and mapping of the human Slc14a2 gene. Am. J. Physiol. Renal Physiol. **281:**F400–F406.
4. **Bagnasco, S. M., T. Peng, Y. Nakayama, and J. M. Sands.** 2000. Differential expression of individual UT-A urea transporter isoforms in rat kidney. J. Am. Soc. Nephrol. **11:**1980–1986.
5. **Bankir, L., K. Chen, and B. Yang.** 2004. Lack of UT-B in vasa recta and red blood cells prevents urea-induced improvement of urinary concentrating ability. Am. J. Physiol. Renal Physiol. **286:**F144–F151.
6. **Fenton, R. A., C. L. Chou, G. S. Stewart, C. P. Smith, and M. A. Knepper.** 2004. Urinary concentrating defect in mice with selective deletion of phloretin-sensitive urea transporters in the renal collecting duct. Proc. Natl. Acad. Sci. USA **101:**7469–7474.
7. **Fenton, R. A., A. Howorth, G. J. Cooper, R. Meccariello, I. D. Morris, and C. P. Smith.** 2000. Molecular characterization of a novel UT-A urea transporter isoform (UT-A5) in testis. Am. J. Physiol. Cell Physiol. **279:**C1425–C1431.
8. **Fenton, R. A., G. S. Stewart, B. Carpenter, A. Howorth, E. A. Potter, G. J. Cooper, and C. P. Smith.** 2002. Characterization of mouse urea transporters UT-A1 and UT-A2. Am. J. Physiol. Renal Physiol. **283:**F817–F825.
9. **Karakashian, A., R. T. Timmer, J. D. Klein, R. B. Gunn, J. M. Sands, and S. M. Bagnasco.** 1999. Cloning and characterization of two new isoforms of the rat kidney urea transporter: UT-A3 and UT-A4. J. Am. Soc. Nephrol. **10:**230–237.
10. **Klein, J. D., J. M. Sands, L. Qian, X. Wang, and B. Yang.** 2004. Upregulation of urea transporter UT-A2 and water channels AQP2 and AQP3 in mice lacking urea transporter UT-B. J. Am. Soc. Nephrol. **15:**1161–1167.
11. **Knepper, M., and G. Gamba.** 2004. Urine concentration and dilution, p. 599–636. In B. Brenner (ed.), Brenner & Rector's the kidney, 7th ed., vol. 1. Saunders, Philadelphia, Pa.
12. **Lim, S. W., C. Li, B. K. Sun, K. H. Han, W. Y. Kim, Y. W. Oh, J. U. Lee, P. F. Kador, M. A. Knepper, J. M. Sands, J. Kim, and C. W. Yang.** 2004. Long-term treatment with cyclosporine decreases aquaporins and urea transporters in the rat kidney. Am. J. Physiol. Renal Physiol. **287:**F139–F151.
13. **Matsumura, Y., S. Uchida, Y. Kondo, H. Miyazaki, S. B. Ko, A. Hayama, T. Morimoto, W. Liu, M. Arisawa, S. Sasaki, and F. Marumo.** 1999. Overt nephrogenic diabetes insipidus in mice lacking the CLC-K1 chloride channel. Nat. Genet. **21:**95–98.
14. **Nakayama, Y., M. Naruse, A. Karakashian, T. Peng, J. M. Sands, and S. M. Bagnasco.** 2001. Cloning of the rat Slc14a2 gene and genomic organization of the UT-A urea transporter. Biochim. Biophys. Acta **1518:**19–26.
15. **Nielsen, S., J. Terris, C. P. Smith, M. A. Hediger, C. A. Ecelbarger, and M. A. Knepper.** 1996. Cellular and subcellular localization of the vasopressin-regulated urea transporter in rat kidney. Proc. Natl. Acad. Sci. USA **93:**5495–5500.
16. **Olives, B., P. Neau, P. Bailly, M. A. Hediger, G. Rousselet, J. P. Cartron, and P. Ripoche.** 1994. Cloning and functional expression of a urea transporter from human bone marrow cells. J. Biol. Chem. **269:**31649–31652.
17. **Sands, J. M.** 2003. Mammalian urea transporters. Annu. Rev. Physiol. **65:**543–566.
18. **Sands, J. M.** 2004. Renal urea transporters. Curr. Opin. Nephrol. Hypertens. **13:**525–532.
19. **Shayakul, C., C. P. Smith, H. S. Mackenzie, W. S. Lee, D. Brown, and M. A. Hediger.** 2000. Long-term regulation of urea transporter expression by vasopressin in Brattleboro rats. Am. J. Physiol. Renal Physiol. **278:**F620–F627.

20. **Smith, C. P., W. S. Lee, S. Martial, M. A. Knepper, G. You, J. M. Sands, and M. A. Hediger.** 1995. Cloning and regulation of expression of the rat kidney urea transporter (rUT2). J. Clin. Investig. **96:**1556–1563.

21. **Stewart, G. S., R. A. Fenton, W. Wang, T. H. Kwon, S. J. White, V. M. Collins, G. Cooper, S. Nielsen, and C. P. Smith.** 2004. The basolateral expression of mUT-A3 in the mouse kidney. Am. J. Physiol. Renal Physiol. **286:**F979–F987.

22. **Terris, J. M., M. A. Knepper, and J. B. Wade.** 2001. UT-A3: localization and characterization of an additional urea transporter isoform in the IMCD. Am. J. Physiol. Renal Physiol. **280:**F325–F332.

23. **Timmer, R. T., J. D. Klein, S. M. Bagnasco, J. J. Doran, J. W. Verlander, R. B. Gunn, and J. M. Sands.** 2001. Localization of the urea transporter UT-B protein in human and rat erythrocytes and tissues. Am. J. Physiol. Cell Physiol. **281:**C1318–C1325.

24. **Wade, J. B., A. J. Lee, J. Liu, C. A. Ecelbarger, C. Mitchell, A. D. Bradford, J. Terris, G. H. Kim, and M. A. Knepper.** 2000. UT-A2: a 55-kDa urea transporter in thin descending limb whose abundance is regulated by vasopressin. Am. J. Physiol. Renal Physiol. **278:**F52–F62.

25. **Yang, B., L. Bankir, A. Gillespie, C. J. Epstein, and A. S. Verkman.** 2002. Urea-selective concentrating defect in transgenic mice lacking urea transporter UT-B. J. Biol. Chem. **277:**10633–10637.

26. **You, G., C. P. Smith, Y. Kanai, W. S. Lee, M. Stelzner, and M. A. Hediger.** 1993. Cloning and characterization of the vasopressin-regulated urea transporter. Nature **365:**844–847.